process of simulation is not as straightforward as might be wished. First there is the challenge of obtaining appropriate interatomic potentials. Fortunately, simple potential models which neglected polarizability worked well for the Na(I)-β''-alumina structure but will almost certainly be too simplistic for the simulation of more complex β''-aluminas, such as those in which the sodium content has been replaced by various divalent cations.

Then there are more subtle issues. For example, if ordering is known to occur in the system under study, information or at least an insightful guess about the superlattice repeat unit must be known a priori so as to avoid a simulation box size that will frustrate the ordering. Detailed knowledge of the crystal structure is also important. Although previously suggested in the literature, this work is the first to explicitly demonstrate that the Mg(II) distribution in the spinel blocks apparently does affect the placement and conductivity of the mobile Na(I). Unfortunately, MD does not provide a way of determining which Mg(II) distribution is correct, thus making the results obtained in this work valid only with respect to the chosen spinel configuration.

Finally, the simulations must be run for a long enough time to allow any correlated motion to be observed. Had the simulations of Na(I)-β''-alumina been run for only 1000 time steps, the low-temperature correlated motion observed after 6000 time steps would have been missed. Long simulations require plentiful computer time, which may not always be available. Nevertheless, once the groundwork is established and a generous computing facility located, MD can be an excellent aid to understanding experimental data. This is clear in our simulation results showing an apparent change in the mechanism of ionic conductivity in Na(I)-β''-alumina from a vacancy mechanism at high temperatures to highly correlated superlattice motion at lower temperatures.

Acknowledgment. This work was supported by the Office of Naval Research and the National Science Foundation, MRL program, under Grant No. DMR-8819885. All simulations were performed on the Pittsburgh Supercomputing Center Y-MP or a Stardent Titan provided by the Laboratory for Research on the Structure of Matter (NSF-MRL) at the University of Pennsylvania. We express our gratitude to M. Zendejas and J. O. Thomas for many useful discussions.

Registry No. Na(I)-β''-alumina, 110619-69-7; aluminum magnesium sodium oxide, 56780-19-9.

Lithium-MVO_5 (M = Nb, Ta) Bronzes

Jose-Manuel Amarilla,† Blanca Casal,† Juan-Carlos Galvan,‡ and Eduardo Ruiz-Hitzky*,†

Instituto de Ciencia de Materiales de Madrid, CSIC, Serrano 115 bis, 28006 Madrid, Spain, and Centro Nacional de Investigaciones Metalúrgicas, CSIC, Gregorio del Amo 8, 28040 Madrid, Spain

Received April 10, 1991. Revised Manuscript Received September 23, 1991

Mixed oxides $NbVO_5$ and $TaVO_5$ have been synthesized by a sol-gel procedure. Both compounds are isostructural with the so-called "monophosphate tungsten bronzes" (MPTB, $(PO_2)_4(WO_3)_{2m}$, with $m = 2$). In such structures single MO_4 tetrahedra (M = P, V), share corners with $M'O_6$ octahedra (M' = W, Ta, Nb) building pentagonal tunnels along the [010] direction. In this work, we have studied lithium insertion redox reactions carried out by treatments with LiI in acetonitrile in MVO_5 (M = Nb, Ta) hosts. Lithium insertion appears as a topotactic and reversible process. The intercalated compounds constitute a new family of Li bronzes showing Li_xMVO_5 compositions with $0 < x < 0.3$, which have been characterized by X-ray diffraction, conventional chemical analysis, and X-ray photoelectron spectroscopy. Complex impedance spectroscopy reveals the ionic character of the electrical conductivity in Li_xMVO_5. Typical values of the specific conductivity are in the 10^{-6}-10^{-8} Ω^{-1} cm^{-1} range at 573 K, with activation energies on the order of 0.5 eV.

Introduction

Transition-metal oxides are extensively applied as component materials in a wide diversity of electronic devices due to their semiconducting, superconducting, and ionic conducting properties. Of particular interest are those oxides able to act as host lattices for alkali-metal (Li, Na) ions, because they can be used as electrode materials in solid-state batteries and as specific sensors. Certain oxides in which the metal element have d^0 electronic configuration (i.e., group V metals) show intrinsic insulating or semiconducting properties, whereas partial reduction of the lattice and/or inclusion of electron donors (i.e., alkali-metal ions) into the host lattice can change drastically their electronic properties.[1] On the other hand, the coexistence of two or more metals in the composition of the oxide matrix can provide an advantage, because the associated electronic structure can improve the resulting properties with respect to those of the parent oxides.[2]

In a previous work,[3] we have shown the potential application of the sol-gel methods to the synthesis of a new crystalline phase in the system Nb-V-O, characterized as $NbVO_5$. We have extended this sol-gel method to the synthesis of $TaVO_5$, isostructural with $NbVO_5$, as discussed

† Instituto de Ciencia de Materiales de Madrid.
‡ Centro Nacional de Investigaciones Metalúrgicas.

(1) Rao, C. N. R.; Gopalakrishnan, J. *New Directions in Solid State Chemistry*; Cambridge solid state science series; Cambridge University Press: Cambridge 1986.
(2) Longo, J. M.; Horowitz, H. S. Solid State Synthesis of Complex Oxides. In *Preparation and Characterization of Materials*; Honig, Rao, Eds.; Academic Press: New York, 1981.
(3) Amarilla, J. M.; Casal, B.; Ruiz-Hitzky, E. *Mater. Lett.* 1989, *8*, 132.

0897-4756/92/2804-0062$03.00/0

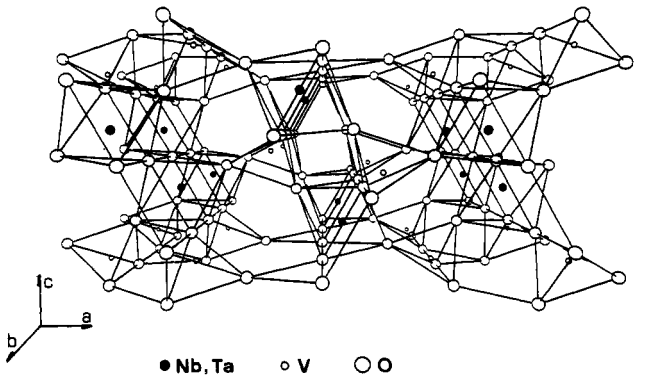

Figure 1. Projection of the structure of MVO_5 oxide (M = Nb, Ta) along the [010] direction.

in this paper. These mixed metal oxides are isostructural with the family of monophosphate tungsten bronzes $[(PO_2)_4(WO_3)_{2m}]$ with $m = 2$.[4-8] The structure of these compounds is built up of corner-sharing VO_4 tetrahedra and $(Nb,Ta)O_6$ octahedra. The most salient structural feature is the presence of pentagonal and rhomboidal channels along the [010] direction (Figure 1). Therefore, one can expect that these materials may be suitable for insertion of metal ions, such as Li^+, into the empty channels.

Our main interest is the synthesis of the Li_xMVO_5 bronzes of both mixed oxides (M = Nb, Ta). These materials are attractive due to their potential applications as cathode materials in solid-state batteries. We will apply impedance spectroscopic measurements for characterizing the electrical behavior of the lithium insertion compounds.

Experimental Section

1. Synthesis of $TaVO_5$ and $NbVO_5$. $NbVO_5$ was synthesized according to a procedure already described.[3] The method of synthesis of $TaVO_5$ is similar to that described for $NbVO_5$. In Scheme I a flowchart corresponding to the preparation of the Ta–V mixed oxide by a sol–gel route is shown. A solution of water/isopropyl alcohol with 1:10 molar ratio was slowly pumped (1 mL/min) into a 1:100 isopropyl alcohol solution of $TaCl_5$ (Fluka, 99.9%) in N_2 atmosphere with constant stirring. After total addition of water/isopropyl alcohol solution, appropriate amounts of a solution 1:100 vanadyl tri-*tert*-butoxide ($[(CH_3)_3CO]_3VO$, prepared as described in ref 3) in isopropyl alcohol was slowly added (1 mL/min). This addition sequence was selected in view of the different hydrolysis rates of these reagents. The whole system was maintained under 63% relative humidity at 295 K, until the formation of a yellow opaque gel was observed (approximately 12 h). The gel was dried at room temperature for 3 days to yield a brown xerogel, which gives crystalline $TaVO_5$ after heating in a platinum crucible at 773 K for 6 h.

2. Lithium Insertion. Lithium insertion in MVO_5 (M = Nb, Ta) mixed oxides was carried out by treatment with LiI/acetonitrile solutions at 373 K in an autogenic Teflon reactor. All manipulations were done in a drybox under controlled atmosphere (N_2). In this way undesirable secondary reactions were avoided, in particular with atmospheric CO_2, which generates insoluble lithium salts.

Procedure I: 25 mL of a saturated solution of LiI (Fluka, 98%) in acetonitrile was added to 0.5 g of the mixed oxide. The resulting mixture was kept in an autogenic reactor, which was maintained at 373 K. After the time periods specified in Figure 3, aliquots were removed from the autoclave, filtered, and washed with acetonitrile until complete elimination of the characteristic iodine color.

Scheme I

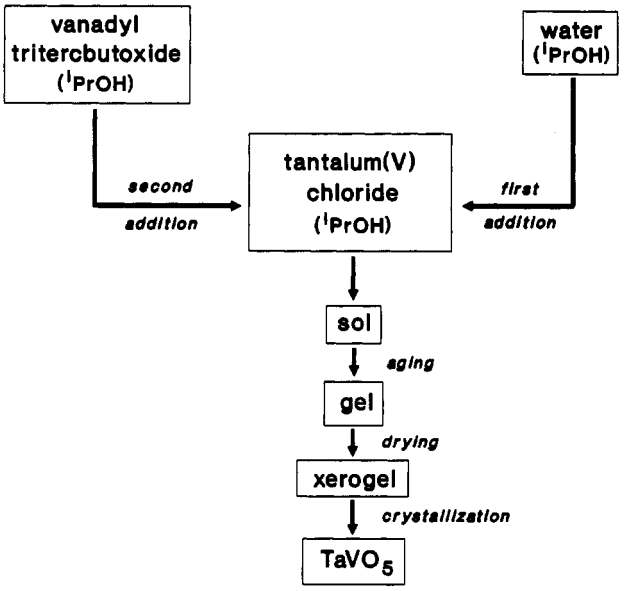

Procedure II: This is similar to procedure I, but after each extraction of aliquots, a proportional amount of the initial solution was added to the system, in order to minimize the reversibilities of the insertion process (see eq 1).

Procedure I was applied to obtain Li bronzes of both MVO_5 (M = Nb, Ta) mixed oxides, whereas procedure II was used to synthesize Li_xTaVO_5 bronzes.

The evolution of the insertion degree with the time of treatment was followed by spectrophotometric measurements of the lithium content in the solid samples.

The reversibility of the insertion process was determined by treating the Li bronze with an excess of I_2/acetonitrile solution at 300 K, under continuous magnetic stirring. To remove all the Li inserted, in the case of ($Li_{0.18}NbVO_5$) bronze, the use of an autogenic reactor thermally treated at 373 K was required.

Characterization. MVO_5 mixed oxides and Li_xMVO_5 bronzes (M = Nb, Ta) were characterized by X-ray powder diffractometry (Philips PW 1710 instrument equipped with a Cu anode and Ni filter), IR spectroscopy (Perkin-Elmer 580B spectrophotometer; KBr pellets), SEM-EDX analyses (Zeiss Model DSM-950, EDX Tracor-Northem Model Z-II instrument), and XPS spectroscopy (Vacuum Generator ESCA LAB MKII spectrometer; radiation Mg Kα (E = 1253.6 eV) or Al Kα (E = 1486.6 eV)); the signals of V_{2p}, Nb_{3d}, and Ta_{4f} have been used to characterize the oxidation state of these elements in the starting and inserted samples.

Ac impedance measurements were carried out at temperatures ranging from 423 to 723 K, with a frequency response analyzer (FRA, Solartron 1174) coupled to an electrochemical interface (Solartron 1286). The applied signal amplitude was 50 mV in the frequency range 1 MHz–10 mHz. Cylindrical disk (area = 0.56 cm^2, thickness = 0.11 cm) samples, previously sintered at 573 K, were placed in a Pyrex cell provided with a platinum grid as current collector. By silver sputtering on the two opposite flat surfaces of the sample, two identical electrodes were formed.

Results and Discussion

Following the method described in the Experimental Section, a series of amorphous xerogel precursors were prepared by sol–gel from vanadyl tri-*tert*-butoxide and niobium or tantalum pentachloride mixtures in isopropyl alcohol (Scheme I). Spots and average SEM-EDX analyses of these precursors show good homogeneity, giving a M/V (M = Nb, Ta) molar ratio close to 1. Subsequent thermal treatment of the M–V xerogels at 873 K for 6 h gave crystalline products identified by XRD as $NbVO_5$ and

(4) Giroult, J. P.; Goreaud, M.; Labbé, P.; Raveau, B. *Acta Crystallogr.* **1981**, *B37*, 2139.
(5) Chahboum, H.; Groult, D.; Hervieu, M.; Raveau B. *J. Solid State Chem.* **1986**, *65*, 331.
(6) Chahboum, H.; Groult, D.; Raveau B. *Mater. Res. Bull.* **1988**, *23*, 805.
(7) Kinomura, N.; Hirose, M.; Kumada, N.; Muto, F. *J. Solid State Chem.* **1988**, *77*, 156.
(8) Wang, S. L.; Wang, C. C.; Lii, K. H. *J. Solid State Chem.* **1989**, *82*, 298.

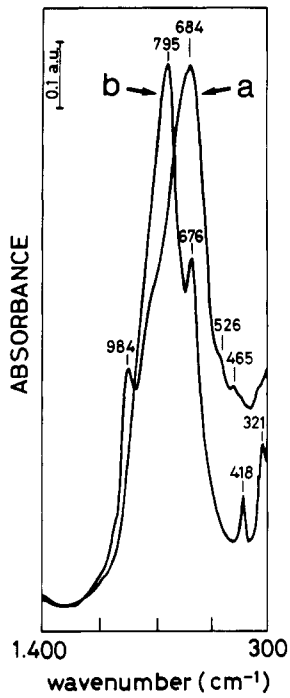

Figure 2. IR spectra (1400–300 cm^{-1} region) of the xerogel precursor (a) and of the $TaVO_5$ crystalline oxide (b).

$TaVO_5$ (refs 3 and 6, respectively).

Characterization of the amorphous precursor and crystalline $NbVO_5$ mixed oxide has been previously reported.[3] In Figure 2 the IR spectra of both the xerogel precursor (a) and the crystalline $TaVO_5$ compound (b) are shown. The spectrum of the latter (b) is similar to that described by Chahboum et al.,[6] whereas spectrum (a) is appreciably different, showing an intense broad band centered at about 684 cm^{-1}. This band can be assigned to stretching (M–O) vibrations in the polymeric mixed oxides.[9-11] The band at 984 cm^{-1}, which dissapears after thermal treatment, could be attributed to stretching metal–oxygen vibrations of remaining short bonds (like V=O) existing in the starting reagent (vanadyl tri-*tert*-butoxide). The development of the intense band at 795 cm^{-1} in the crystalline phase of $TaVO_5$ (b) suggests that the structural $[VO_4]$ tetrahedra (Figure 1) are distorted, as was also evidenced by ^{51}V NMR solid-state spectroscopy in $NbVO_5$.[12] This band is also observed, but as a shoulder, in the xerogel (a), indicating the heterogeneity in the structural coordination in which vanadium atoms are arranged in the amorphous precursor.

Lithium Inclusion. Chemical inclusion of Li^+ ions into MVO_5 (M = Nb, Ta) was carried out according to eq 1.

$$MVO_5 + xLiI \leftrightarrow Li_xMVO_5 + x/2I_2 \quad (1)$$

This is a redox reaction in which the iodide ions act as a reducing agent of the transition-metal ions of the host lattice; thus, lithium ions are inserted in the solid, balancing the net charge of the system.

Appreciable changes of color (from yellow to dark-gray) occur with the progress of the reaction. Similar behavior is also observed in other transition-metal oxides (WO_3, MoO_3, V_2O_5, etc). This is of great interest for applications in electrochromic devices.[13] The mechanism of coloration

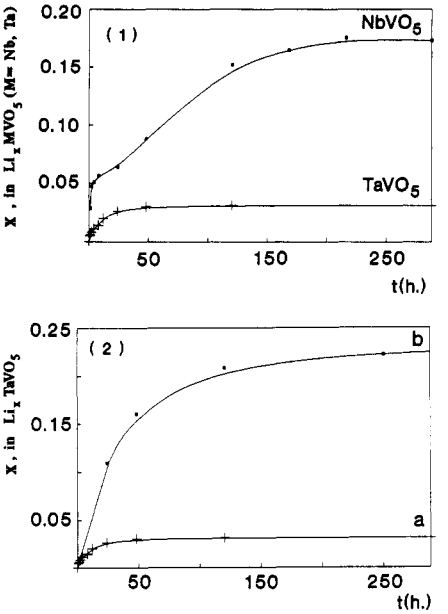

Figure 3. (1) Time evolution of the lithium insertion reactions for the materials $NbVO_5$ and $TaVO_5$. (2) Time evolution of the lithium insertion reactions for $TaVO_5$ oxide without (a) or with (b) changes of the initial lithium iodide/acetonitrile solution.

is ascribed to the simultaneous injection of electrons with the compensating cations (i.e., Li^+) in the host lattice. In contrast, any changes were observed in the corresponding X-ray patterns after lithium inclusion, showing the topochemical character of the process. Wang and Greenblatt[14] describe the chemical intercalation of alkali-metal ions (Li, Na) in the structurally related compounds $[(PO_2)_4(WO_3)_{2m}]$, for values of $m \geq 4$. In these cases, the Li/W ratio is close to 2, with lithium ions basically located in the cubooctahedral cavities of the $(WO_3)_n$ slabs. In the MVO_5 (M = Nb, Ta) compounds, where $m = 2$, such cubooctahedral cavities do not exist, and the location of inserted Li^+ ions must be limited to the pentagonal channels or to the rhombohedral tunnels (Figure 1).

The time evolution of the insertion reactions (Figure 3) shows that the lithium insertion degree increases with respect to the reaction time, reaching a "plateau" that depends on both the nature of the elements in the oxide and the experimental conditions: in this figure are shown the differences in the lithium insertion degree in samples of $NbVO_5$ and $TaVO_5$ (Figure 3.1), obtained without (Figure 3.2.a) or with (Figure 3.2.b) changes of the initial lithium iodide/acetonitrile solutions, as described in the Experimental Section (procedures I and II, respectively). The successive change of the initial solution (procedure II) minimizes the reversibility of the process (eq 1) enhancing the insertion reaction. In this way a Li bronze of $Li_{0.22}TaVO_5$ composition is obtained working at 373 K (7 days). However, experiments performed without removing the supernatant (procedure I) gave a compound of lower lithium content ($Li_{0.03}TaVO_5$). In the case of $NbVO_5$, with procedure I, the degree of lithium inclusion is about 0.2 lithium/formula, comparable to that obtained for the $TaVO_5$ oxide following the more drastic conditions (procedure II). This fact does not have an easy explanation considering (i) the topochemical character of the inclusion reaction and (ii) the similar ionic radii of Nb and Ta in octahedral coordination,[15] which determines a priori the

(9) Baran, E. J.; Escobar, M. E. *Spectrochim. Acta* **1985**, *41A*, 415.
(10) Dartiguenave, M.; Dartiguenave, Y. *Bull. Soc. Chim. Fr.* **1968**, 171.
(11) Abe, M. *Inorganic ion exchange materials*; Clearfield, Ed.; CRC Press: Boca Raton, FL, 1982.
(12) Davis, J.; Tinet, D.; Fripiat, J. J.; Amarilla, J. M.; Casal, B.; Ruiz-Hitzky, E. *J. Mater. Res.* **1991**, *6*, 393.
(13) Bange, B.; Gambke, T. *Adv. Mater.* **1990**, *2*, 10.
(14) Wang, E.; Greenblatt, M. *J. Solid State Chem.* **1987**, *68*, 38.
(15) Shannon, R. D.; Prewitt, C. T. *Acta Crystallogr.* **1969**, *B25*, 925.

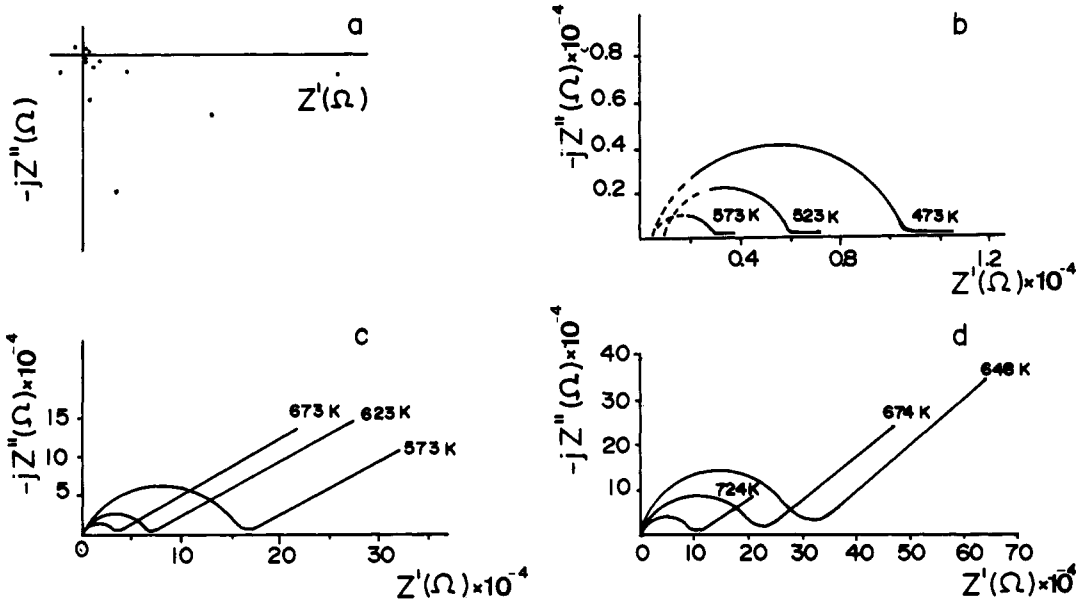

Figure 4. Impedance spectra (Nyquist plots) for $TaVO_5$ (a), $Li_{0.18}$ $NbVO_5$ (b), $Li_{0.22}$ $TaVO_5$ (c), and $Li_{0.03}$ $TaVO_5$ (d).

Table I. Analysis (%) by XPS for the MVO_5 (M = Nb, Ta) Oxides and Their Li_xMVO_5 Bronzes

sample	V^{5+}	V^{4+}	Nb^{5+}	Ta^{5+}
$TaVO_5$	79	21	100	
$Li_{0.03}TaVO_5$	75	25	100	
$NbVO_5$	76	24		100
$Li_{0.18}NbVO_5$	62	38		100

Table II. Lithium Desintercalation for the Li_xMVO_5 (M = Nb, Ta) Bronzes

	lithium desintercalation, %	
Li bronze	I_2/acetonitrile, room temp, stirring, 7 days	I_2/acetonitrile, in reactor, 373 K, 7 days
$Li_{0.18}NbVO_5$	33	95
$Li_{0.03}TaVO_5$	70	

similar size and sections of the structural channels. At this point, we thought that vanadium and niobium atoms in the host lattice of $NbVO_5$ could be affected, during the first steps of the inclusion reaction, by the reduction process induced by the LiI, whereas the tantalum, in the structure of $TaVO_5$, did not. This hypothesis could also explain the two plateaus observed at the kinetic curve of $NbVO_5$. Nevertheless, an evaluation by XPS measurements of the M^{4+}/M^{5+} (M = Nb, Ta) ratio at the surface of the samples before and after the lithium intercalation (Table I), indicates that neither niobium nor tantalum are reduced during the reaction. Thus, we must conclude that the stability of $TaVO_5$ toward the reducing agent is greater than that of the $NbVO_5$, at least in the initial step of the reaction. It is noteworthy that the stability toward Li insertion of the MVO_5 (M = Nb, Ta) mixed oxides is greater than that of V_2O_5. Thus, $Li_xV_2O_5$ bronzes ($0 \leq x \leq 1$) are easily formed by LiI/acetonitrile treatments at room temperature.[16] On the other hand, more active reducing agents (i.e., *n*-butyllithium/hexane) are required to reach high insertion degrees (approximately 1 Li/metal) in other vanadium/niobium or tantalum mixed oxides as VM_9O_{25} (M = Nb, Ta),[17] which show a structural arrangement of vanadium ions closely related to MVO_5. The use of more active agents, as *n*-butyllithium in hexane at room temperature (24 h), produces significant damages in the original MVO_5 structure, giving amorphous materials.

In agreement with the structure established from the X-ray powder diagrams[6] and the ^{51}V high-resolution NMR study,[12] MVO_5 mixed oxides are orthovanadates, whereas the XPS analysis (Table I) indicates that a fraction of vanadium is originally reduced at the surface of the host matrix, probably due to residual isopropyl alcohol able to act as a reducing agent during the thermal treatment in the mixed oxides preparation. After Li insertion, the increase of the quantity of reduced V^{5+} deduced from the XPS (surface) is close to the Li amount determined by conventional chemical analysis of the samples (bulk) suggesting a homogeneous composition of the bronzes.

Table II shows the degree (percent) of reversibility of the lithium insertion reaction (eq 1) in both $Li_{0.03}$ $TaVO_5$ and $Li_{0.18}$ $NbVO_5$ bronzes. In both cases, high lithium desinsertion levels are reached, without changes in the corresponding X-ray diffraction patterns. The original color of the host matrices is recovered; this behavior is attributed to the changes in the oxidation state of vanadium of the host lattice with the insertion–desinsertion processes. These results show that the lithium insertion processes are reversible in these bronzes.

Electrical Properties. Figure 4 shows the complex impedance spectra of the $TaVO_5$ host sample as well as those corresponding to the $Li_{0.18}$ $NbVO_5$, $Li_{0.03}$ $TaVO_5$, and $Li_{0.22}$ $TaVO_5$ bronzes, respectively. The host material, $TaVO_5$, lacks electrical conductivity in the measured temperature range, which produces a dispersion of points in the Nyquist diagram (Figure 4a), also observed for the $NbVO_5$ oxide. In the case of the $Li_{0.18}$ $NbVO_5$ (Figure 4b), a semicircumference appears in the corresponding diagram, which can be interpreted by an equivalent circuit composed of a resistance (R_i) and a capacitance (C_g) in parallel. The discontinuous lines in the Nyquist plot represent a dispersion of points at high frequencies, probably due to limitations in the measuring equipment. Nevertheless, it has been possible to determine the controlling stage of the electrical transport process in the solid, by the impedance values in medium- and low-frequency zones.

At high frequencies, for the Li_xTaVO_5 ($x = 0.03$ or 0.22) bronzes, the Nyquist plots show well-described semicir-

(16) Murphy, D. W.; Christian, P. A.; DiSalvo, F. J.; Waszczak, J. V. *Inorg. Chem.* **1979**, *18*, 2801.
(17) Cava, R. J.; Murphy, D. W.; Zahurak, S. M. *J. Electrochem. Soc.* **1983**, *130*, 2345.

Table III. Calculated Values, from the Nyquist Diagrams, for the Geometric Capacitance, C_g, Permittivity, ϵ', Resistence, R_i, and Specific Conductivity, σ_i, of the Li_xMVO_5 (M = Nb, Ta) Bronzes (T = 573 K)

sample	10^{11} C_g, F	ϵ'	R_i, kΩ	σ_i, $(\Omega\ cm)^{-1}$
$Li_{0.18}NbVO_5$	4.62	62.28	27.8	3.5×10^{-6}
$Li_{0.22}TaVO_5$	1.27	17.78	157.9	7.8×10^{-7}
$Li_{0.03}TAVO_5$	0.38	9.13	1215.0	8.0×10^{-8}

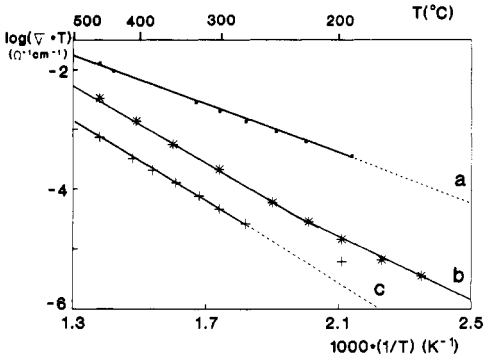

Figure 5. Plots of log (σT) versus $1/T$ (K^{-1}) for the $Li_{0.18}$ $NbVO_5$ (a), $Li_{0.22}$ $TaVO_5$ (b), and $Li_{0.03}$ $TaVO_5$ (c) bronzes.

cumferences, whereas in the domain of low frequencies, straight lines appear with slope close to 1. This observation is explained by a modification of the equivalent circuit by addition of a new element, the Warburg impedance (Z_w), in series with the resistance R_i and in parallel with the capacitance C_g.[18]

Table III shows the values calculated for the geometric capacitance, C_g, permittivity, ϵ', and specific conductivity, σ_i, of the bronzes at 573 K, obtained from the corresponding Nyquist diagrams.[18,19] In all cases, the values of the C_g fall within the range 10^{-11}–10^{-12} F, which according to Irvine et al.[20] is associated with a capacitance whose dielectric properties are due to a phenomena controlled by the bulk material, rather than other effects such as grain boundary, sample/electrode interface, etc. Likewise, an independence of C_g and ϵ' from the temperature, shows the constancy in the physical and chemical nature of the materials in all ranges of temperature studied. On the other hand, the low values obtained from the capacitance are indicative of the lack of any contribution related to electronic transport.[21]

According to the equivalent circuit proposed, in parallel with the capacitance there is a resistance, R_i, physically associated with the resistance of the lithium ions migration through the structural channels of the bulk, assuming that these cations are the electrical charge carriers. Specific electrical conductivities, σ_i, were calculated from the experimental resistances and the geometric dimension of the pellets[22] (Table III).

For ionic conductors, the dependence between specific conductivity and temperature is given by the Arrhenius expression in the form

$$\log \sigma_i T = \log A - 0.434E_a/RT \qquad (2)$$

Table IV. Activation Energy for Ionic Conduction Process in the Li_xMVO_5 Bronzes (M = Nb, Ta)

Li bronze	E_a, kJ/mol	temp range, K
$Li_{0.22}TaVO_5$	51.4	423–515
	62.9	515–723
$Li_{0.03}TaVO_5$	62.5	523–723
$Li_{0.18}NbVO_5$	38.4	473–723

in which E_a is the activation energy involved in the transport process, A is a constant, and R and T are the gas constant and the absolute temperature, respectively. Figure 5 shows the Arrhenius plots for the different samples studied. Generally a linear relationship is observed between $1/T$ and log ($\sigma_i T$); in the $Li_{0.22}$ $TaVO_5$ bronze (Figure 5b) the slope of the plot changes at around 515 K, whereas in the other bronzes such change is not defined probably due to the absence of experimental data in this temperature region. Considering the hypothesis that lithium ions are located in the structural channels of the solid this change in the slope would imply that, above a defined temperature, lithium ions are able to move through the two types of the structural channels. A similar interpretation has been described by Gregorkiewitz[23] in feldespathoid type materials. Slope changes of the log ($\sigma_i T$) vs $1/T$, in differents polyphosphates,[24] have been recently interpreted as a modification in the charge carrier (Li^+) number with the temperature, without invoking crystal structure modifications.

As is known, there is a direct relationship between the number of charge carriers and the ionic conductivity of the materials. Thus, we can explain the differences found in the ionic conductivity of the Li_xTaVO_5 (x = 0.03 and 0.22) bronzes, observing that this one increases as the lithium content increases. This fact supports the idea that the lithium ions are responsible for the electrical-transport process.

The comparative study of the bronzes $Li_{0.22}$ $TaVO_5$ and $Li_{0.18}$ $NbVO_5$ can also be of interest, due to their structural analogies and the similar amounts of inserted lithium. Both materials have similar conductivities ($Li_{0.18}$ $NbVO_5$ slightly higher) showing that the transport process does not depend on the transition metal (Ta, Nb) included in the host lattice. This result is in line with the relative chemical analogies of Ta and Nb.

Table IV shows the values of the activation energies for the ionic conductivity process in the studied bronzes. In general, the obtained values are all of the same order of magnitude. They are comparable to the values described in the bibliography for good lithium ion conductors.[24] The similar values obtained for the activation energies in the $Li_{0.22}$ $TaVO_5$ bronzes, for temperatures above 515 K, and the $Li_{0.03}$ $TaVO_5$ indicate that the structure of the host material in not affected by insertion of lithium ions, in accordance with the conclusion reached by the XRD technique, showing the topotactic character of the lithium insertion process. On the other hand, the activation energy at this temperature range suggest that the mechanism of the ionic conduction is identical in the two Li_xTaVO_5 bronzes (x = 0.03, 0.22).

For the $TAVO_5$ bronzes, besides the semicircumference, a straight line appears at low frequencies (Warburg tail, Figure 4c,d), associated with a diffusion process;[22] therefore, in these cases we must suppose a mixed mechanism: diffusion conduction plus ionic transport. Unlike ionic conduction, which is exclusively produced by the gradient

(18) Casal, B.; Ruiz-Hitzky, E.; Crespin, M.; Tinet, D.; Galván, J. C. *J. Chem. Soc., Faraday Trans. 1* **1989**, *85*, 4167.
(19) Macdonald, J. R. *Impedance spectroscopy: emphasizing solid materials and systems*; Macdonald, J. R., Ed.; Wiley: New York, 1987.
(20) Irvine, J. T. S.; Sinclair, D. C.; West, A. R. *Adv. Mater.* **1990**, *2*, 132.
(21) West, A. R. *Solid State Chemistry and its Applications*; Wiley: Chichester, 1984.
(22) Oliveira, A. L.; Damasceno, O. O.; Oliveira, J.; Schouler, E. J. L. *Mater. Res. Bull.* **1986**, *21*, 877.
(23) Gregorkiewitz, M. *Solid State Ionics* **1986**, *18–19*, 534.
(24) El Horr, N.; Hammou, A.; Bagieu, M. *J. Solid State Chem.* **1991**, *90*, 361.

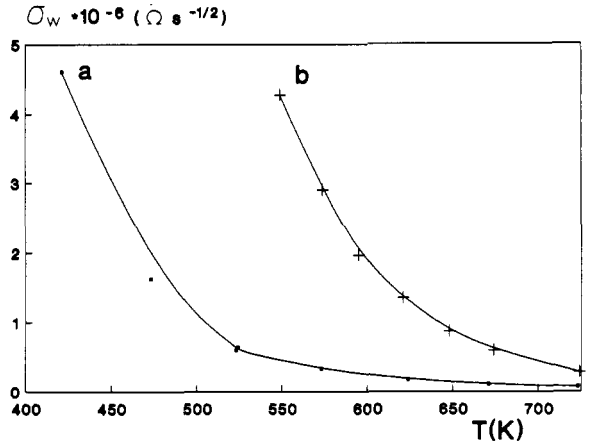

Figure 6. Temperature dependence of Warburg's coefficient for $Li_{0.22}$ $TaVO_5$ (a) and $Li_{0.03}$ $TaVO_5$ (b) bronzes.

of potential created by the applied electrical signal, diffusion takes place by the existence of a gradient of concentration, caused either by the effect of the imposed sinusoidal signal or by inhomogeneities of the material. At the highest frequencies, only the fastest processes are developed (ionic transport and polarization), whereas at the lowest frequencies all the processes can be observed (diffusion and ionic conduction).

Warburg's impedance, Z_w, is defined by the expression

$$Z_w = \sigma_w(1 - j)/\sqrt{\omega} \tag{3}$$

where ω is the frequency of the applied electrical signal and σ_w is the Warburg diffusion coefficient, defined as

$$\sigma_o = \frac{RT}{\sqrt{2n^2F^2}} \frac{1}{C\sqrt{D}} \tag{4}$$

$$D = D_0 e^{Q/RT} \tag{5}$$

where D is the chemical diffusion coefficient of the controlling diffusion species, C represents its concentration in the bulk, n, is the number of transferred charges, F is the Faraday constant, D_0 is a factor which comprises various constants, including the vibrational frequency of the carriers, and Q is the activation energy of diffusion.

Figure 6 shows the temperature dependence of the Warburg coefficient for the Li_xTaVO_5 bronzes (x = 0.22 and 0.03), respectively. Three aspects are worthy of note: (i) in both cases, a large decrease of σ_w is observed with the temperature; (ii) $Li_{0.22}$ $TaVO_5$ presents, at the same temperature, lower values of the Warburg coefficient than $Li_{0.03}$ $TaVO_5$; (iii) the σ_w values approach a plateau at the highest temperatures. Regarding point i, the decrease of σ_w with temperature, which implies larger values for the diffusion coefficient (eq 4), can be explained by an increase of the thermal activation, which favors the beginning and development of the ionic diffusion movement. Regarding point ii, in accordance with eq 4, σ_w is inversely related to the bulk concentration of electroactive species. Thus, the lower value of σ_w for $Li_{0.03}$ $TaVO_5$ is consistent with eq 4. Finally, the plateau in Figure 6 at high temperature suggests that the crystalline structure of the bronzes allows the lithium ions to move freely through the material above

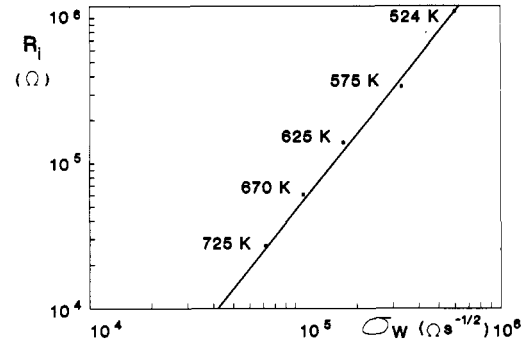

Figure 7. Relationship between the ionic resistivity and the Warburg's coefficient for $Li_{0.22}$ $TaVO_5$ bronze.

a critical temperature. Thus, the analysis of the experimental results strongly support lithium ions as the main species responsible for the transport processes in these materials.

It is interesting to note the close relationship existing between ionic conductivity and the values of the Warburg coefficients. Figure 7 shows the variations of the log R_i vs log σ_w, for $Li_{0.22}$ $TaVO_5$. We observe that these parameters evolve almost identically with temperature, which can be interpreted by a noticeable increase of transport barriers as the temperature is lowered. This behavior suggests that the ionic conductivity and the Warburg coefficient (associated with the diffusion process) depend on the same phenomenon: the ability of the ions to move along the structural channels of the solid.

Conclusions

Sol–gel methods allow for the synthesis of new $NbVO_5$ mixed oxide and appears as an alternative route to prepare $TaVO_5$. These oxides show interesting structural features, such as the presence of channels with pentagonal and rhomboidal sections along the [010] direction, which allow for the insertion of lithium ions. Thus, a novel family of Li bronzes can be prepared by redox processes involving chemical reactions between the MVO_5 oxides and LiI dissolved in acetonitrile. Lithium insertion appears as a topotactic and reversible process. This interesting property opens a way for potential future applications in the field of electronic devices (cathode batteries, electrochromic materials, etc.). Electrical conductivity of the Li bronzes studied by impedance spectroscopy reveals suitable values for the activation energy (less than 0.5 eV), although the number of charge carriers (Li^+) is relatively low. More active reducing chemical reagents, as n-butyllithium, or electrochemical lithium insertion are currently being studied in our laboratory in order to enhance the amount of Li in the Li_xMVO_5 bronzes.

Acknowledgment. We are very grateful to Dr. Crespin (CRSOCI, CNRS, Orleans, France) for his assistance in the XPS measurements. This work was partially supported by the CICYT of Spain (Project MAT 725/90); J.M.A. was subsidized by a grant from the Ministerio de Educacion y Ciencia of Spain.

Registry No. $NbVO_5$, 12201-62-6; $TaVO_5$, 16452-69-0; Li, 7439-93-2; $Li_{0.03}TaVO_5$, 137125-14-5; $Li_{0.18}NbVO_5$, 137125-15-6; $Li_{0.22}TaVO_5$, 137125-16-7.